

OPTICAL AND THERMAL PROPERTIES OF CdF<sub>2</sub>-BASED GLASSES FOR 1.3 μm  
Pr-DOPED OPTICAL FIBRE AMPLIFIERS

A.JHA<sup>⊗</sup>, M.NAFTALY<sup>⊗</sup>, S.JORDERY<sup>⊗</sup>, B.SAMSON\*, D.W. HEWAK\* & D.N. PAYNE\*

<sup>⊗</sup> Department of Materials Technology, Brunel University,  
Kingston Lane, Uxbridge, Middlesex UB8 3PH, U.K.

\* Optoelectronics Research Centre, University of Southampton,  
High Fields, Southampton, Hampshire SO9 5NH, U.K.

ABSTRACT

Cadmium mixed halide glasses exhibit lower peak phonon energy than conventional fluorozirconate glasses. New glass compositions doped with Pr<sup>3+</sup>-ions were fabricated using controlled atmosphere melting and casting techniques. The optical properties of new bulk glasses were studied by spectroscopic techniques. The significance of an empirically-derived total loss curve for bulk glass is examined for the design of a 1.3 μm amplifier. The concentration effects of Pr<sup>3+</sup>-ions as a dopant in the glass were studied, and its absorption cross-section measured to establish the ground state absorption in bulk glass. The thermal stability of mixed halide glasses was studied by differential scanning calorimetry, and an appraisal of their devitrification behaviour is presented.

INTRODUCTION

The evolution of broad band communication in silica fibre passive optical networks (PONs) followed the development of single mode fibres. Consequently, the past few years have seen an unprecedented change in the capabilities of optical fibre communications. Whitley et al<sup>(1)</sup> recently pointed out that the point-to-point transmission system circa 1990 utilised state-of-the-art electrical-to-optical and vice versa conversion of 1550 nm signals at the transmitter and receiver ends respectively. Evidently, conversion of electromagnetic waves from one form to another is a non-trivial operation. Problems arise when data transmission rates exceed 2.5 Gbit/sec; also the span length for signal regenerators is only 70 km. The first optical fibre laser was demonstrated by Koester and Snitzer<sup>(2)</sup>, but it was only recently in 1985 that Mears et al<sup>(3)</sup> demonstrated a low-noise erbium-doped fibre amplifier operating at 1540 nm, providing a solution for the replacement of electronic regenerators. The device, as has been predicted<sup>(4)</sup>, will be suitable for repeaterless transmission in transoceanic submarine cable networks. The majority of global land-based optical communication, however, operates at the second transmission window of silica, at 1300 nm wavelength; the first and third windows in silica are situated at 850 nm and 1550 nm respectively. An optical amplifier for the 1300 nm wavelength domain is not available, and therefore the development and demonstration of the device is of utmost importance for the future strategies of network management and operation.

In a 1300 nm optical amplifier, fluorescence occurs when Pr-ions dispersed in glass are optically excited to the <sup>1</sup>G<sub>4</sub> level using a 1000 nm pump. The scheme for the 1300 nm transition is shown in *Figure 1*, where the ion excitation and relaxation processes are designated by steps A, B, C and D. Using this scheme, within the space of a few months three different research groups announced their results with Pr-doped fluorozirconate fibres having a quantum efficiency of about one percent<sup>(5-7)</sup>; more recently however, a slightly better efficiency has been reported<sup>(8)</sup> in a similar system. The poor quantum efficiency of the 1300 nm Pr-doped fluoride optical fibre amplifier results from the large multiphonon relaxation rate that is related to the phonon energy (ħω) of the rare-earth ion host. The phonon energy of the fluorozirconate host is 580 cm<sup>-1</sup> and is attributed to the nc

bridging fluorine vibrations in the glass structure. This is just over half of the phonon energy of a silica host, which is  $1120\text{ cm}^{-1}$ . The latter is therefore unsuitable, as its quantum efficiency value is several orders of magnitude smaller than the values observed in fluorozirconate glasses. An important indicator of both high gain and quantum efficiency of Pr-ions in a host is the fluorescence lifetime ( $\tau$ ) of the metastable state, the  ${}^1G_4$  level, from which Pr-ions relax radiatively to the lower  ${}^3H_5$  level by emitting light of 1300 nm wavelength. The larger the phonon energy of the host, the shorter is the metastable lifetime of Pr-ions, due to the large probability of a non-radiative relaxation to the underlying  ${}^3F_4$  level. In order to prolong the metastable lifetime of Pr-ions at the  ${}^1G_4$  level, and hence improve the gain and quantum efficiency, the phonon energy of the host must be lowered. Recently, we reported a number of possible low phonon-energy glass hosts suitable for doping with Pr-ions<sup>(9)</sup>; cadmium mixed halide is one such family of glasses having a maximum phonon energy ( $\hbar\omega$ ) of  $\sim 380\text{ cm}^{-1}$ <sup>(10)</sup>. The glass has also attractive preform-forming and fibre fabrication characteristics, owing to the large difference in the values of the onset of crystallisation ( $T_c$ ) and the glass transition ( $T_g$ ) temperatures.

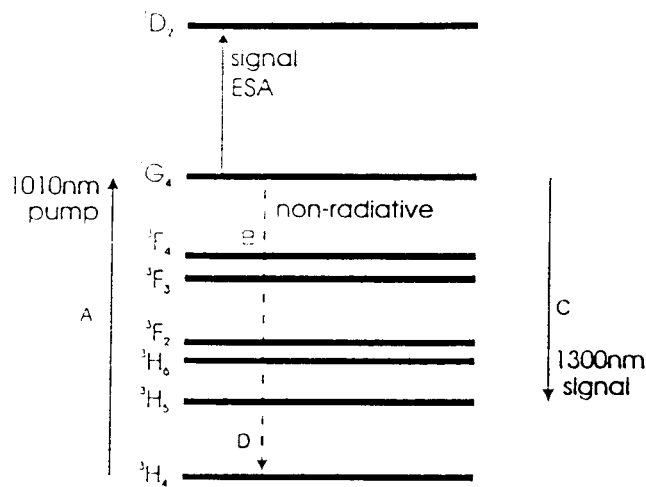


Figure 1: Partial energy-level diagram of Pr-ion

Invoking the relationship between the number of phonons ( $p$ ), the phonon energy  $\hbar\omega$  ( $\sim 380\text{ cm}^{-1}$ ) and the  ${}^1G_4$ - ${}^3F_4$  energy gap in praseodymium ( $\Delta E$ ), we clearly find that the cadmium mixed halide glass will require twice the number of phonons to bridge the energy gap,  $\Delta E$ , of  $2960\text{ cm}^{-1}$  than a fluorozirconate glass. Consequently a significant reduction in phonon relaxation rate is expected, facilitating a longer metastable lifetime than the  $100\text{ }\mu\text{sec}$  observed in fluorozirconate glasses for the  $1.3\text{ }\mu\text{m}$  transition. It is for this reason that we have selected the cadmium mixed halide glass host for the 1300 nm optical fibre amplifier. When considering amplifier design, it is important to characterise the absorption and emission features of the rare-earth doped bulk glass and the drawn fibres. The gain of an optical fibre amplifier can be depleted through one of the following processes or via their combination: a) *multiphonon relaxation and concentration quenching*, b) *excited state absorption (ESA)*, c) *amplified stimulated emission (ASE)*, and d) *ground state absorption (GSA)*.

Multiphonon relaxation in Pr-doped glasses, as described above, is a dominant process whereas, unlike in neodymium, the ASE and ESA are less important. Ion-ion cross-relaxation (concentration quenching) begins to dominate at increased concentrations, leading to a significant loss of pump energy and hence resulting in poor gain and quantum efficiency. GSA is important because Pr-ions absorb signal photons due to their non-zero extinction coefficient; it should be minimised by a compositional modification of host. A selected few results are shown below. Both cross-relaxation and GSA are strongly concentration dependent. In the first part of the present paper we will examine the effects of Pr-ion extinction coefficient ( $\epsilon$ ) in the cadmium mixed halide glass host. Following this, we report the values of the multiphonon absorption edge ( $\alpha_{mp}$ ) in these glasses and the computed Rayleigh scattering ( $\alpha_r$ ) curve; these two are combined to construct a V-shaped loss curve. The loss of signal energy due to the total intrinsic loss,  $\alpha_t$  (dB/km), which is the sum of  $\alpha_{mp}$  and  $\alpha_r$ , is also estimated. Finally we will also present the thermal properties of the bulk glass, which can be utilised to predict the ease of preform and fibre fabrication, particularly for single mode fibre fabrication.

## EXPERIMENTAL RESULTS AND DISCUSSION

The cadmium mixed halide composition is based on the system  $CdX_2-MX_2-M'X_2$ , where X is a halide ion. M and M' are divalent and monovalent ions from Group IIA and IA of the periodic table. Cadmium halide used was 99.9 weight percent pure and required further purification. The effect of purification on the IR absorption spectra of cast bulk glass samples, prepared in a dry glove box, is reported in *Figure 2*. The possible impurity absorption peaks were identified and are listed in *Table 1*. A typical thickness of a clear crystal-free glass sample was 5 mm; this was also used as an indicator of the glass-forming ability in the mixed halide system. The cast bulk glass doped with different concentrations of Pr-ion was polished in a suitable non-aqueous medium, which could be either dry ethanol or methanol, to achieve surface quality acceptable for IR absorption measurements.

Table 1: List of identified impurities and their peak wavenumbers ( $cm^{-1}$ ).

OH <sup>-1</sup>	Surface water	Carbonate	Nitrate	Sulphate	Oxide
3700-2000	1600	1320-1530	1018-1050	1210-1040	1050-1000

The absorption measurements for Pr-ions were carried out using a Perkin-Elmer Lambda-19 UV-VIS-NIR spectrophotometer. Absorption in the vicinity of pump and signal wavelengths of the 1300 nm amplifier was also determined and is shown in *Figure 3*. The value of  $\epsilon$  at 1.3  $\mu m$  was separately determined in two different samples doped with 500 ppm and 1000 ppm and was found to be 0.23 and 0.6 dB/km/ppm respectively. The higher of these values gives value for  $\sigma_a$  of  $1.35 \times 10^{-22} cm^2$ . This determines the absorption of signal photons, as given by the equation:  $I_s(x) = I_s(0) \exp(-\alpha_s x)$ , where  $\alpha_s$  is equal to the product ( $N_p \sigma_s$ ) and x is the waveguide length in centimetres. In *Figure 4*, the GSA in fluorozirconate (ZBLAN) is compared with that in cadmium mixed halide. The GSA in mixed halide is slightly higher than in ZBLAN.

The intrinsic absorption is a combination of Rayleigh scattering and the multiphonon absorption edge. The latter is determined by using the Lambert-Beer equation<sup>(11)</sup> shown above for signal energy absorption. The multiphonon absorption edge is shown in *Figure 5* together with the computed Rayleigh scattering curve. The method of computation adopted for  $\alpha_R$  is similar to that described elsewhere<sup>(11)</sup>. From this figure, we conclude that the value of intrinsic loss at pump and signal wavelengths is less than  $10^{-4}$  dB/m. This value however may be unrealistic to achieve in practice, particularly in fibre geometry, owing to fabrication defects and impurity absorption. So far, from our preliminary fibre drawing trials, unacceptably high values of loss have been measured (8-15 dB/m); these are attributed to extrinsic defects and crystallisation.

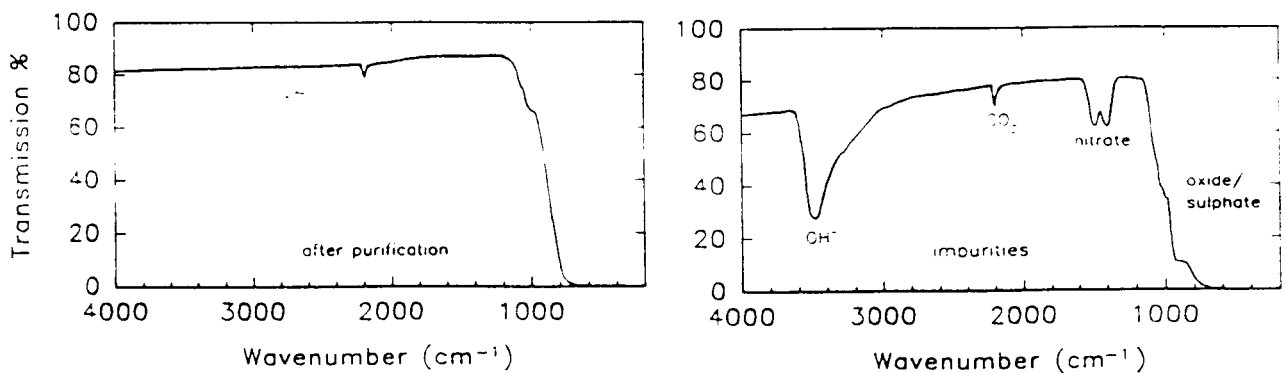


Figure 2: IR spectra of mixed halide glass before and after purification

In a previous publication, we reported<sup>(10)</sup> that the relative intensities of Cd-F and Cd-Cl vibrations in the glass structure are dependent upon the concentrations of the exchangeable anions. In the present case, the exchange occurs between M or M' chlorides and cadmium fluorides<sup>(12)</sup>. The ratio of integrated intensities of Cd-Cl and Cd-F is equal to 3:1. This ratio can also be compared with our results based on the thermodynamic analysis for an equimolar concentration of CdF<sub>2</sub> and MCl<sub>2</sub> or M'Cl. The CdCl<sub>2</sub>-MF<sub>2</sub> combination is 22% more energetically probable than a purely random distribution, giving the predicted ratio of 72:28. The calculation also illustrates the reason for the addition of MX<sub>2</sub> and M'X in the mixed halide melt. The overall configurational entropy of the melt reduces due to a preferential formation of (Cd-Cl)-like structural units in the liquid state, hence improving the glass-forming ability. **Table 2** shows some significant optical properties of cadmium mixed halide glasses. The values of both  $h\omega$  and  $\Delta E$  indicate that the number of phonons involved in the multiphonon relaxation process could be as many as 8 or greater. Our Judd-Ofelt analysis<sup>(9)</sup> indicates that the radiative lifetime of the <sup>1</sup>G<sub>4</sub> level could also be large. We have noted that impurities play a critical role in shortening the <sup>1</sup>G<sub>4</sub> fluorescence lifetime: the disparity between the predicted and the measured lifetimes is attributed to the presence of impurities. The longest lifetime so far achieved is 320  $\mu$ sec, yielding a quantum efficiency (QE) of 13%. This is better than the value currently observed in ZBLAN-type glasses.

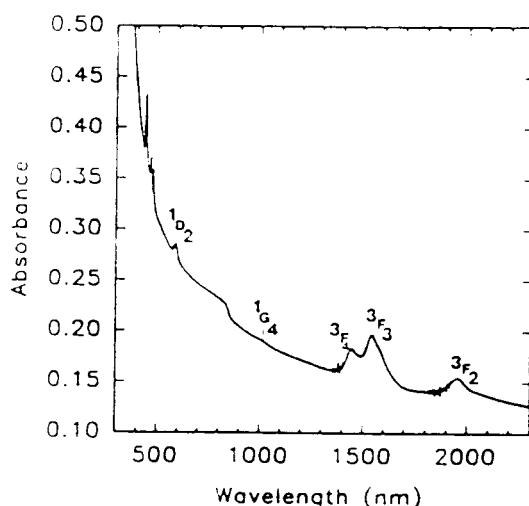


Figure 3: Absorption spectrum of Pr-Ion in mixed halide glass

Table 2: Optical properties of cadmium mixed halide glasses.

980  
2870

Energy, cm <sup>-1</sup>		n <sub>D</sub>	Lifetimes, $\mu$ sec			QE
$\Delta E$	$h\omega$		$\tau_{rad}$	$\tau_{mp}$	$\tau_{max}$	%
2970	240	1.592	2460	3720	320	13

Small glass fragments were also collected and transferred into gold pans for differential scanning calorimetric (DSC) analysis. All necessary precautions were heeded to avoid moisture contamination of thermal analysis samples. For this, the sample loading procedure in a dry atmosphere, preferably a melting glove box, is recommended. The characteristic temperatures  $T_g$ ,  $T_x$  and the onset of principal melting event ( $T_m$ ) were determined by using the isochronal heating method, and these are 135°, 230° and 305°C respectively. Two glass stability parameters are presented that indicate the tendency for devitrification and crystallisation during reheating and cooling of undercooled halide melts; these are designated as  $H_R$  and  $S$  parameters respectively. The value of  $H_R$  equals to  $(T_x - T_g)/(T_m - T_x)$ , and  $S$  is defined by the equation  $S = ((T_x - T_g)(T_p - T_x))/T_g(°C)$ . Here  $T_p$  is the peak crystallisation temperature. The derived value of  $H_R$  and  $S$  varies between 1.2-1.8 and 5.5-9.0 (°C) respectively.  $H_R$  consists of two terms namely,  $(T_x - T_g)$  and  $(T_m - T_x)$ . The numerator determines the nucleation rate which decreases with the increasing value of the gap. This means that a wider gap will significantly hinder the nucleation of crystals that will subsequently grow. The driving force for the crystal growth, however, is determined by the denominator, i.e. the  $(T_m - T_x)$  gap. The narrower the gap becomes, the slower is the growth of crystals.

Indeed, it is for this reason that a large value of  $H_R$  is preferred for both preform fabrication and fibre drawing. On the other hand, the  $S$  parameter is a better indicator of fibre drawing conditions. This is because the parameter is defined by only those thermal events that occur before melting, i.e. the glass devitrification peak. The kinetics of devitrification, defined by both nucleation and crystal growth, is dependent on the  $(T_x - T_g)$  and  $(T_p - T_x)$  terms. The rate at which a glass recrystallises during isothermal and isochronal heating can be qualitatively established by determining the peak width i.e.  $(T_p - T_x)$ . As the peak width increases, the crystal growth rate during the devitrification process drops rapidly. It is for this reason that most oxide network-forming glasses exhibit excellent resistance to devitrification on heating above their transition temperatures ( $T_g$ ).

The coefficient of thermal expansion of the glass varies with composition, and for the range of compositions we have covered the value varies in the range  $210\text{-}245 \times 10^{-7}/^\circ\text{C}$ .

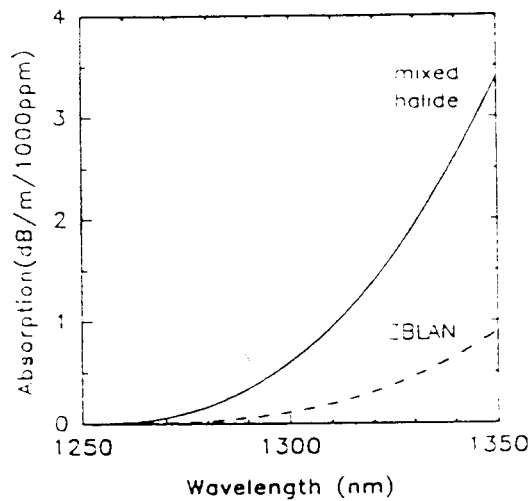


Figure 4: GSA in Pr-doped mixed halide and ZBLAN glass hosts

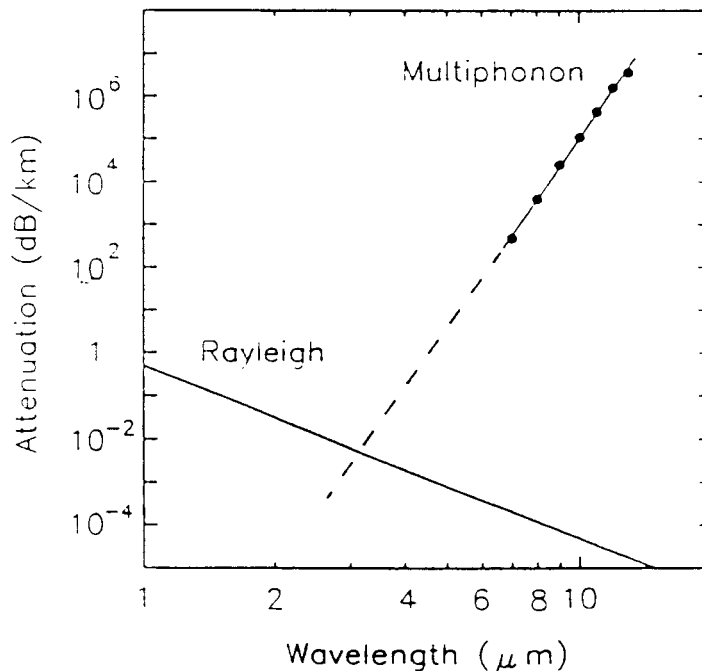
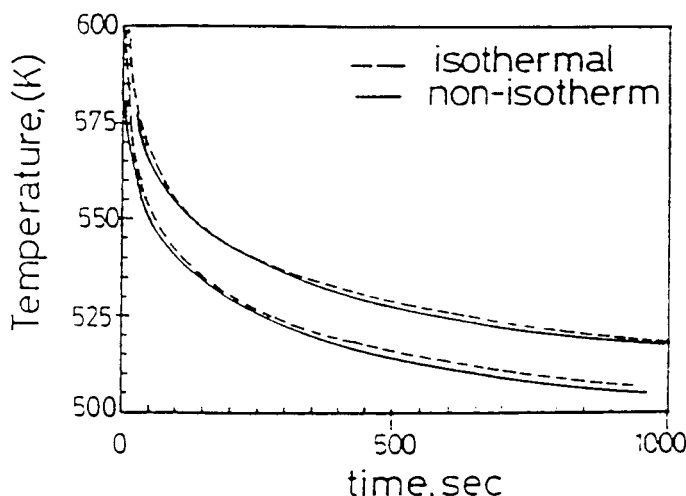


Figure 5: Multiphonon absorption edge and computed Rayleigh scattering in the mixed halide glasses

The isochronal heating method, discussed by Clavaguera-Mora et al<sup>(13)</sup>, was also employed to study the rate of devitrification. The results were used to construct a time-temperature-transformation (t-t-t) curve for the reheating of glass samples. This is shown in *Figure 6*, and indicates that the glass exhibits a thermal stability superior to that of most fluorozirconate compositions. The t-t-t curve is consistent with the stability parameters defined above which are an indirect reflection of nucleation and crystal growth rates during devitrification as well as during the cooling of undercooled melts. Combined with superior optical properties, we anticipate that the mixed halide optical fibres will be a more efficient 1.3  $\mu\text{m}$  amplifier than the ZBLAN glass fibre-based device.



*Figure 6: Time-temperature-transformation curve for a mixed halide glass.*

## CONCLUSIONS

The spectroscopic studies suggest that cadmium mixed halide glasses are a potential glass-forming system for the Pr-ion as dopant. The thermal properties point to favourable preform making and fibre drawing conditions.

## ACKNOWLEDGEMENTS

Authors acknowledge financial support from EEC/RACE and the Science and Engineering Research Council, UK for the project on Fluoride Glass Optical Fibre Amplifiers and Lasers.

## REFERENCES

- 1) T. Whitley, R. Wyatt, D. Szebesta and S. T. Davey : British Telecom Technology Journal, **11** (1993) pp.115-127.
- 2) C. J. Koester and E. Snitzer: Appl. Optics, **3** (1964) 1182.
- 3) R. J. Mears, L. Reekie, S. B. Poole and D.N. Payne: Electron. Lett. **21** (1985) 738.
- 4) W. A. Gambling: Science and Engineering Research Council Bulletin, **4** (1993) pp.20-21.
- 5) S.F. Carter, D. Szebesta, S. T. Davey, R. Wyatt, M.C. Brierly and P.W. France: Electron Lett. **27** (1991) pp.628-629.
- 6) Y. Durteste, M. Monerie, J. Y. Allain and H. Poignant: *ibid*, pp. 630-631.
- 7) Y. Ohishi, T. Kanamori, T. Kitagawa, S. Takahashi, E. Snitzer and G. H. Sigel: Optics Letters, **16** (1991) pp.1747-1749.
- 8) Y. Miyajima, T. Sugawa and Y. Fukusaku: Electron Lett. **27** (1991) 1706.
- 9) D. W. Hewak et al: *ibid*, **29** (1993) pp. 237-239.
- 10) R. S. Deol et al: J. Non-crystalline Solids, 1993 (in press).
- 11) W. G. Jordan, A. Jha and J. L. Ryan: J. Materials. Sci. Lett., **11** (1992) pp.771-773.
- 12) A. Jha and J. M. Parker: Phys. Chem. Glasses, **32** (1991) pp.1-12.
- 13) M. T. Clavaguera-Mora, M. D. Baro, S. Surinach and N. Clavaguera: J. Mater. Res., **5** (1990) pp.1201-1206.